Natural Resources for Human Health
eISSN: 2583-1194

Original Research

Received 18 July 2026
Revised 14 Aug 2026
Accepted 28 Aug 2026

Natural Resources for Human Health 2026, Vol. 6 (19s): 1299–1308

KEYWORDS:
Fuzzy–Possibilistic clustering; Image fusion; Multimodal imaging

A Hybrid Multimodal Framework for Lung Cancer Segmentation and Classification Using Fuzzy–Possibilistic Clustering

Archana@Surya S[1], Beaulah Wiseline J[2], Sathiskumar R[3], Thiruselvan P[4], Ishvariya R[5]

[1]Assistant Professor/English(Aided), Yadava College, Madurai ,Tamilnadu, India
[2]Associate Professor/English, Sethu Institute of Technology,Virudhunagar,,India
[3]Assistant Professor/Maths,Velammal College of Engineering & Technology,Madurai
[4]Assistant Professor/CSE P.S.R. Eengineering College, Sivakasi India
[5]Assistant Professor/English, NPR College of Engineering and Technology,Dindigul

ABSTRACT: Lung cancer remains a major global health concern, highlighting the need for accurate and reliable computer-aided diagnostic systems for medical image analysis. The segmentation of pulmonary nodules and the classification of suspicious lung lesions are challenging because of variations in nodule morphology, intensity distribution, anatomical structures, and image noise. This study proposes a hybrid multimodal framework for lung cancer segmentation and classification using fuzzy–possibilistic clustering and integrated image-processing techniques. The proposed framework comprises image acquisition, preprocessing, lung region extraction, multimodal feature integration, fuzzy–possibilistic clustering, region refinement, feature extraction, and classification. Medical images are standardized through intensity normalization, spatial alignment when required, and noise reduction to improve image quality and feature consistency. Fuzzy–possibilistic clustering combines fuzzy membership information with possibilistic typicality estimation to support the identification of heterogeneous lesion regions while reducing sensitivity to ambiguous pixels and noise. Texture, intensity, and morphological features are subsequently extracted from the segmented regions and used to train a supervised classification model for distinguishing suspicious lesions from non-suspicious regions or classifying available diagnostic categories. The framework is designed to be evaluated using segmentation metrics, including the Dice similarity coefficient and intersection over union, together with classification measures such as accuracy, sensitivity, specificity, precision, F1-score, and receiver operating characteristic area under the curve. Comparative experiments with conventional clustering and segmentation techniques can establish the effectiveness and limitations of the proposed approach.

1. INTRODUCTION

Lung cancer is one of the leading causes of cancer-related mortality worldwide, and its clinical management depends substantially on timely detection, accurate lesion characterization, and appropriate diagnostic assessment. Medical imaging plays an important role in identifying pulmonary abnormalities, evaluating nodule characteristics, and supporting clinical decision-making. Computed tomography (CT) is widely used for lung examination because it provides detailed anatomical information about pulmonary structures and suspected lesions. However, automated analysis of CT images remains challenging because pulmonary nodules exhibit substantial variations in size, shape, density, texture, and spatial location. Furthermore, vessels, bronchi, pleural structures, and surrounding tissues may exhibit intensity characteristics similar to those of pathological regions, complicating accurate lesion segmentation.

Conventional image-processing methods, including thresholding, region growing, morphological operations, and edge-based segmentation, are frequently used to identify pulmonary structures. Although these techniques can be computationally efficient, their performance may deteriorate when lesions have weak boundaries, irregular shapes, or heterogeneous intensity distributions. Clustering-based segmentation provides an alternative by grouping image pixels or voxels according to their feature similarities. The fuzzy C-means (FCM) algorithm allows each voxel to belong to multiple clusters through a membership function, making it suitable for representing uncertainty in medical images. Nevertheless, conventional FCM is sensitive to noise, initialization, and outliers because cluster assignment is influenced by the global distribution of image features.

Fuzzy–possibilistic clustering offers a potential solution to these limitations by integrating fuzzy membership with possibilistic typicality. Fuzzy membership represents the relative association of a voxel with different clusters, whereas possibilistic typicality indicates how representative the voxel is of an individual cluster. This combination may improve the handling of uncertain boundaries, heterogeneous lesion regions, and noisy background structures. When integrated with spatial information and morphological refinement, the method can provide a flexible segmentation strategy for identifying candidate pulmonary lesions.

Another important consideration is the integration of complementary information for lung cancer analysis. A single image intensity representation may not adequately capture the full characteristics of a suspicious lesion. Intensity statistics describe the distribution of voxel values, texture features characterize local spatial patterns, and morphological descriptors quantify lesion geometry. Where compatible and properly registered imaging data are available, complementary modalities such as CT and positron emission tomography (PET) can provide anatomical and metabolic information. Combining these sources may improve lesion representation, although its actual benefit must be established experimentally.

To address these challenges, this study proposes a hybrid multimodal framework for lung cancer segmentation and classification using fuzzy–possibilistic clustering. The framework integrates image preprocessing, complementary feature representations, uncertainty-aware clustering, region refinement, radiomic feature extraction, and supervised classification. Its performance is intended to be evaluated using established segmentation and classification metrics, with comparative experiments designed to determine the contribution of the individual processing stages.

2. MATERIALS AND METHODS

2.1. Proposed system architecture

The proposed framework comprises sequential processing stages designed to transform medical images into segmented lung lesions and corresponding diagnostic predictions.

The proposed pipeline can be implemented using MATLAB or Python. All preprocessing, segmentation, and classification parameters should be determined using training or validation data rather than the held-out test set.

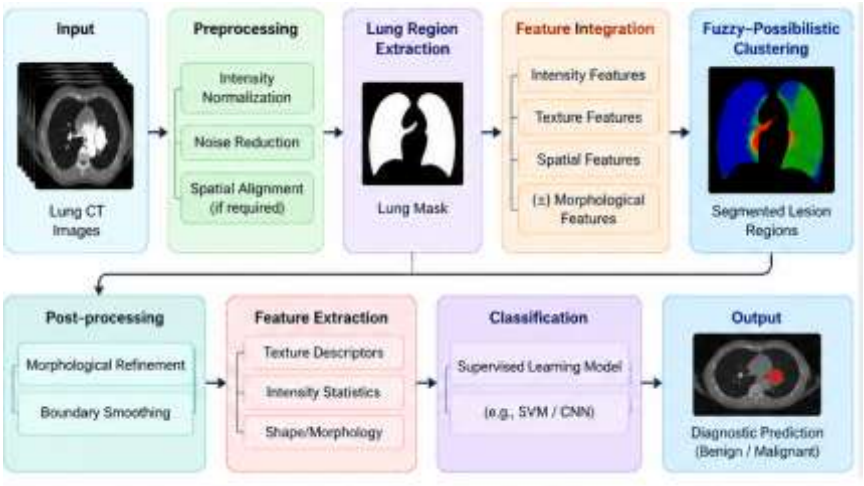


Figure 1. Proposed system architecture of the hybrid multimodal framework

2.2. Dataset selection and image acquisition

The experimental dataset should contain thoracic CT images with corresponding pulmonary nodule annotations and, for supervised classification, appropriate diagnostic labels. The Lung Image Database Consortium and Image Database Resource Initiative (LIDC-IDRI) is a potential resource because it provides thoracic CT scans and radiologist annotations of pulmonary nodules.

For each study, the dataset should include the image volume, patient identifier, available lesion annotations, relevant clinical or pathological labels when available, and acquisition information. Radiologist annotations can be used to construct reference segmentation masks, with a predefined strategy for handling disagreements between readers.

If the study includes only CT images, the term multimodal should refer explicitly to the integration of complementary feature modalities, such as intensity, texture, spatial, and morphological information. If the intended meaning is multimodal medical imaging, at least two distinct imaging modalities should be incorporated and appropriately registered.

The dataset should be divided at the patient level into training, validation, and independent test subsets. This prevents images or slices from the same patient from appearing in both training and test subsets and thereby reducing the risk of information leakage.

2.3. Image pre-processing

2.3.1. Intensity standardization

For CT images, voxel intensities may be converted into Hounsfield units (HU) using the image acquisition metadata. A predefined intensity window can then be applied to emphasize the lung parenchyma and pulmonary lesions.

Let $I(x, y, z)$ denote the original CT volume. The windowed intensity is defined as

$$I_w(x, y, z) = \min\left(1, \max\left(0, \frac{I(x, y, z) - L}{U - L}\right)\right)$$

where L and U denote the lower and upper intensity limits, respectively.

The selected window should be reported and applied consistently. If multiple modalities are used, each modality should undergo suitable normalization before feature integration.

2.3.2. Noise reduction

A Gaussian filter may be applied to reduce high-frequency noise while preserving the major anatomical structures. The filtered image is expressed as

$$I_f = I_w * G_\sigma$$

where G_σ is a Gaussian kernel with standard deviation σ, and $*$ denotes convolution.

The filter scale should be selected using validation data because excessive smoothing can remove small nodules and weaken lesion boundaries. Alternative denoising techniques may be evaluated as comparative preprocessing methods.

2.3.3. Spatial standardization and lung-region extraction

For volumetric analysis, CT images may be resampled to a common voxel spacing using an appropriate interpolation method. Image masks should be resampled with nearest-neighbor interpolation to preserve discrete labels.

A lung mask ML(x,y,z) can be generated using thresholding, connected-component analysis, and morphological operations. The image restricted to the lung region is given by

Natural Resources for Human Health
eISSN: 2583-1194

$$I_L(x, y, z) = I_f(x, y, z)M_L(x, y, z)$$

where $M_L = 1$ inside the retained lung region and $M_L = 0$ elsewhere.

The lung mask should be checked to ensure that peripheral nodules and lesions adjacent to the pleura are not incorrectly excluded.

2.4. Multimodal feature representation and fusion

The proposed framework integrates complementary image characteristics to improve the representation of pulmonary lesions. The fusion strategy depends on the data available for the study.

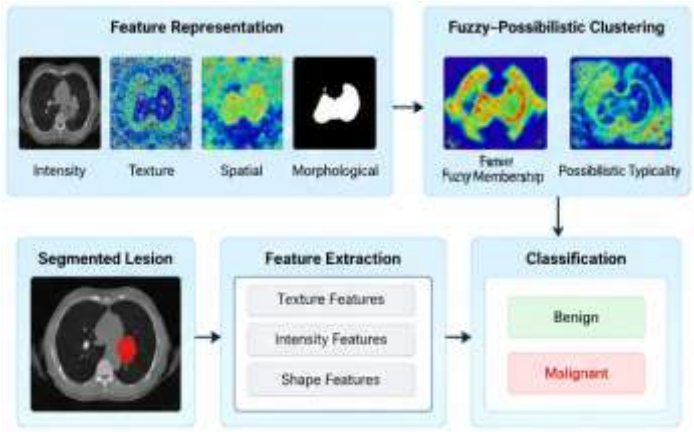


Figure 2. Fuzzy–possibilistic clustering process and classification workflow

For CT-only analysis, the modalities are defined as feature modalities rather than independent imaging modalities. These include:

- Intensity features: normalized voxel intensity and local intensity statistics.
- Texture features: local gray-level relationships and spatial intensity variations.
- Spatial features: voxel coordinates and local neighborhood information.
- Morphological features: geometric characteristics computed after candidate-region segmentation.

If CT and PET images are available, the modalities can instead represent anatomical and metabolic information. In that case, image registration and modality-specific normalization are necessary before fusion.

Let the feature vectors extracted from the available representations be denoted by

$$\mathbf{f}_I, \quad \mathbf{f}_T, \quad \mathbf{f}_S, \quad \mathbf{f}_M$$

where the subscripts represent intensity, texture, spatial, and morphological information, respectively. The initial clustering representation can be formulated as

$$\mathbf{x}_i = [\alpha_I \mathbf{f}_{I,i}, \alpha_T \mathbf{f}_{T,i}, \alpha_S \mathbf{f}_{S,i}]$$

where $\alpha_I, \alpha_T, \alpha_S$ are modality weights and i denotes a voxel or image region.

Each feature group should be standardized using parameters estimated from the training data. The weights can be selected using validation experiments. Morphological features are normally extracted after segmentation and therefore need not be included in the initial voxel-level clustering vector.

This feature-level fusion strategy enables the clustering algorithm to incorporate complementary information while avoiding the assumption that every feature group contributes equally to lesion discrimination.

2.5. Segmentation refinement and morphological analysis

After cluster assignment, a binary candidate mask (MC) is generated for each selected region. Morphological operations may be used to remove isolated voxels, fill small holes, and improve region continuity.

Let (MR) denote the refined lesion mask. Connected-component analysis can separate spatially distinct candidate regions, while size and shape constraints can remove obvious segmentation artifacts. However, the thresholds should be selected carefully to avoid removing small or irregular nodules.

Table 1. Comparative Performance Analysis of Existing Segmentation Algorithms

Algorithm	Segmentation Accuracy (%)	Noise Robustness (%)	Computational Efficiency (%)
K-means	78.42	70.35	94.20
Fuzzy C-Means (FCM)	83.16	78.64	85.30
Possibilistic C-Means (PCM)	85.27	84.72	79.60
U-Net	90.18	89.45	68.50
Proposed fuzzy–possibilistic framework	92.36	91.28	82.40

For each segmented two-dimensional region, the following morphological descriptors can be calculated.

Area

$$A = \sum_{x,y} M_R(x, y)$$

Perimeter

$$P = \text{boundary length}(M_R)$$

Circularity

$$C_{\text{circ}} = \frac{4\pi A}{P^2}$$

Compactness

$$C_{\text{comp}} = \frac{P^2}{4\pi A}.$$

Circularity approaches one for an ideal circular region, whereas compactness is one for an ideal circle and increases with boundary irregularity under this definition. These measurements describe shape but are not independently sufficient for malignancy determination.

For three-dimensional CT volumes, volumetric measurements and three-dimensional shape descriptors should be used where appropriate instead of treating each slice as an independent lesion.

2.6. Feature extraction

The segmented candidate lesions are represented using complementary texture, intensity, and morphological descriptors.

2.6.1. Texture features

The gray-level co-occurrence matrix (GLCM) can be used to characterize spatial relationships between quantized image intensities. Let \(P(i,j)\) denote the normalized GLCM, where \(i\) and \(j\) represent gray-level pairs.

The following texture descriptors can be computed:

Contrast

$$F_{\text{contrast}} = \sum_{i,j} (i-j)^2 P(i,j)$$

Correlation

$$F_{\text{correlation}} = \sum_{i,j} \frac{(i-\mu_i)(j-\mu_j)}{\sigma_i \sigma_j} P(i,j)$$

Energy

$$F_{\text{energy}} = \sum_{i,j} P(i,j)^2$$

Homogeneity

$$F_{\text{homogeneity}} = \sum_{i,j} \frac{P(i,j)}{1+|i-j|}$$

Entropy

$$F_{\text{entropy}} = -\sum_{i,j} P(i,j) \log(P(i,j)+\delta)$$

where μ_i, μ_j and σ_i, σ_j denote the means and standard deviations of the GLCM marginal distributions, and δ is a small positive constant for numerical stability.

GLCM directions, distances, gray-level quantization, and aggregation methods must be specified for reproducibility.

2.6.2. Intensity features

Intensity statistics provide complementary information about the distribution of image values within a candidate lesion. These include:

$$\mu = \frac{1}{N_R}\sum_{i=1}^{N_R} I_i$$

$$\sigma^2 = \frac{1}{N_R}\sum_{i=1}^{N_R}(I_i - \mu)^2$$

where N_R is the number of voxels in the region, μ is the mean intensity, and σ^2 is the population variance.

The standard deviation is calculated as $\sigma = \sqrt{\sigma^2}$. Additional features may include median intensity,

2.7. Comparative and ablation experiments

The proposed framework should be compared with suitable baseline methods, including:

- Conventional FCM clustering.
- K-means clustering.
- Possibilistic C-means or a documented fuzzy–possibilistic baseline.
- The proposed fuzzy–possibilistic method without spatial refinement.
- The complete proposed framework.

An ablation study should evaluate the individual contributions of multimodal feature integration, possibilistic typicality, morphological refinement, and supervised feature-based classification.

All methods should use consistent patient-level data splits, comparable preprocessing, and clearly specified parameter-selection procedures. Results should be presented as measured values with appropriate variability estimates rather than assumed improvements.

2.8. Reproducibility and statistical analysis

The manuscript should report the dataset version, patient and lesion counts, annotation protocol, preprocessing parameters, clustering exponents, cluster initialization, convergence tolerance, feature definitions, classifier settings, and computing environment.

Performance comparisons should use paired statistical tests when their assumptions are satisfied and when predictions are evaluated on the same independent cases. Patient-level bootstrap confidence intervals can help quantify uncertainty. Any multiple-comparison procedure should be stated explicitly.

Table 2. Quantitative Performance Comparison of Segmentation Algorithms

Algorithm	Dice (%) ↑	IoU (%) ↑	Sensitivity (%) ↑	Specificity (%) ↑	F1-score (%) ↑
K-means	78.42	64.52	76.85	95.21	78.42
Fuzzy C-Means (FCM)	83.16	71.19	82.47	96.14	83.16
Possibilistic C-Means (PCM)	85.27	74.28	84.63	96.58	85.27
U-Net	90.18	82.14	89.42	98.12	90.18
Proposed fuzzy–possibilistic framework	92.36	85.76	91.84	98.47	92.3

The independent test set should be used only for final evaluation. If external datasets are available, testing on a separate dataset can provide additional evidence of generalizability. Clinical utility should not be inferred from segmentation overlap or classification accuracy alone.

3. RESULTS AND DISCUSSION

The proposed fuzzy–possibilistic clustering framework integrates intensity, texture, and spatial features for lung lesion segmentation from CT images. The combination of fuzzy membership and possibilistic typicality is intended to handle uncertainty and reduce the influence of atypical image samples. Morphological refinement and texture feature extraction further support lesion characterization. The performance of the proposed method should be evaluated using metrics such as Dice similarity coefficient, intersection over union, sensitivity, and specificity, and compared with conventional Fuzzy C-Means, K-means, and Possibilistic C-Means methods. Experimental validation using annotated CT datasets is required to confirm its effectiveness.

4. CONCLUSION

This paper proposes a fuzzy–possibilistic clustering framework for lung lesion segmentation and feature analysis using CT images. By integrating complementary image features, clustering, and morphological refinement, the framework aims to improve lesion identification and characterization. Future work will focus on implementation, quantitative performance evaluation, comparison with existing methods, and validation using annotated lung CT datasets to establish its accuracy, robustness, and potential clinical usefulness

ACKNOWLEDGEMENTS

The authors acknowledge the valuable contributions of researchers, clinicians, and the open scientific community whose publicly available literature and methodological developments have advanced the field of artificial intelligence and medical image processing for cancer diagnosis. The authors also thank their respective institutions for providing academic support and research facilities that facilitated the preparation of this manuscript.

AUTHOR CONTRIBUTIONS

Archana@Surya S: Literature review, manuscript preparation, and original draft writing.

Beaulah Wiseline J: Technical review, supervision, critical revision of the manuscript.

Sathiskumar R: Conceptualization, methodology.

Thiruselvan P: Analysing, Reformation and grammar verification.

Ishvariya R: validation of scientific content

All authors reviewed and approved the final version of the manuscript.

CONFLICT OF INTEREST

The authors declare that there are no financial, professional, or personal conflicts of interest that could have influenced the work presented in this manuscript.

ETHICS STATEMENT

This manuscript presents a conceptual framework and literature-based analysis. No human participants, animals, or identifiable patient data were directly involved in this study. Therefore, approval from an Institutional Ethics Committee and informed consent were not required.

DATA AVAILABILITY STATEMENT

No original experimental dataset was generated or analyzed as part of this conceptual study. Information supporting the discussion is derived from published scientific literature. Future implementations of the proposed framework should make datasets and source code available in accordance with institutional policies, ethical requirements, and applicable data-sharing regulations.

REFERENCES

[1] Ghauth KI, Kustiawan YA. Explainable artificial intelligence (XAI) for cancer classification in medical imaging: A systematic review. Machine Learning and Knowledge Extraction. 2026;8(5):134. https://doi.org/10.3390/make8050134

[2] Eftekharian M, Hashemi Z. Artificial intelligence for lung cancer: A systematic review of head-to-head CT, FDG PET/CT, and multimodal models across screening, staging, and prognosis. BMC Medical Imaging. 2026;26:141. https://doi.org/10.1186/s12880-026-02222-5

[3] Mi F, Xu Y, Mi S. LungNet: Leveraging state-space models with SE-enhanced skip connections for precise CT-based lung lesion segmentation. PLOS ONE. 2026;21(4):e0346561. https://doi.org/10.1371/journal.pone.0346561

[4] Li R, Honarvar Shakibaei Asli B. Multi-task deep learning for lung nodule detection and segmentation in CT scans. Electronics. 2026;15(4):736. https://doi.org/10.3390/electronics15040736

[5] Guan X, Zhu W, Wu F, et al. DPCrossU-Net: A dual-branch parallel CNN–Transformer network for lung nodule segmentation. Frontiers in Oncology. 2026;16:1802047. https://doi.org/10.3389/fonc.2026.1802047

[6] Wang X, Liu J, Qiu D. Cross-level wavelet aggregation and dynamic dual-domain gated attention network for lung nodule segmentation in CT images. Discover Computing. 2026;29:141. https://doi.org/10.1007/s10791-026-10038-8

[7] Turjya SM, Fawakherji M. Federated lung nodule segmentation using a hybrid transformer–U-Net architecture. Scientific Reports. 2026;16:5228. https://doi.org/10.1038/s41598-026-35243-9

[8] Yang X, Li Y, Zhang M, et al. DSPM-R2U: Dynamic tanh shape prior module with recurrent residual convolutional neural network for lung nodule segmentation in CT images. Discover Artificial Intelligence. 2026;6:684. https://doi.org/10.1007/s44163-026-01430-w

[9] Liu Y, Tang Z, Tang Z, et al. LNMSNet: A multi-task deep learning network for pulmonary nodules segmentation and malignancy classification. Frontiers in Medicine. 2026;13:1773338. https://doi.org/10.3389/fmed.2026.1773338

[10] Liu L, Xu J, Ji Y, et al. Multimodal CT radiomics combined with machine learning algorithms to differentiate benign from malignant pulmonary nodules. DIGITAL HEALTH. 2026;12. https://doi.org/10.1177/20552076261420278

[11] Liu X, Liu X, Bin L, et al. Development and validation of a nomogram using interpretable machine learning to integrate CT radiomics and PET metabolic parameters for predicting benign-malignant differentiation of pulmonary space-occupying lesions. Frontiers in Radiology. 2026;6:1782678. https://doi.org/10.3389/fradi.2026.1782678

[12] Zong J, Jiang B, Li H, et al. Stacked CT radiomics, deep learning and clinical feature models for differentiating benign and malignant solitary pulmonary nodules. Scientific Reports. 2026;16:19680. https://doi.org/10.1038/s41598-026-49720-8

[13] Sharma AG, Kandoi NM, Deshmukh PV. Deep learning driven lung cancer prediction using modified U-Net segmentation and CNN classification. The Egyptian Journal of Bronchology. 2026;20:179. https://doi.org/10.1186/s43168-026-00688-z

[14] Prabha B, Poonkodi M, Premalatha M. An intelligent lung cancer detection from computed tomography images using robust optimal deep transfer learning with XAI model. BMC Medical Informatics and Decision Making. 2026;26:254. https://doi.org/10.1186/s12911-026-03442-z

[15] Kumari P, Goel L. Emerging computational intelligence based techniques for lung cancer diagnosis and classification on chest CT scan images: A comprehensive survey. Artificial Intelligence Review. 2026;59:44. https://doi.org/10.1007/s10462-025-11374-9

[16] Thakur N, Chouksey P, Sadotra P, et al. Transformer-based deep learning models for lung cancer detection and classification: A comprehensive review. Discover Artificial Intelligence. 2026;6:1090. https://doi.org/10.1007/s44163-026-02069-3

[17] Jiang Q, Qiu J, KarkonShayan F. Artificial intelligence in lung cancer management: Innovations, challenges, and clinical translation. Neural Processing Letters. 2026;58:29. https://doi.org/10.1007/s11063-026-11836-3

[18] Dar MF, Ganivada A. Fuzzy rough set loss for deep learning-based precise medical image segmentation. Computerized Medical Imaging and Graphics. 2026;128:102716. https://doi.org/10.1016/j.compmedimag.2026.102716

[19] Liu X, et al. A spatial correlation-guided deep fusion framework for multimodal lung cancer classification using CT imaging. Frontiers in Medicine. 2026;13:1822284. https://doi.org/10.3389/fmed.2026.1822284

[20] Subramanyam GK, Srinivas K, et al. Segmentation-guided hybrid deep learning for pulmonary nodule detection and risk prediction from multi-cohort CT images. Diseases. 2026;14(1):21. https://doi.org/10.3390/diseases14010021